Journal of Geography and Social Sciences, 2021, 3 (1), 17-30.
http://www.jgss.com.pk

Original Article OPEN ACCESS

Computing Spatio-temporal variations in land surface temperature: A case study of Tehsil Murree, Pakistan

Naqia Gull [1], Muhammad Adeel [2], Liaqat Ali Waseem [1], Dostdar Hussain [3], Nasir Abbas [4], Adnan Elahi [1], Zawwar Hussain [5], Bulbul Jan [6], Muhammad Nasar-U-Minallah [7], Syed Ali Asad Naqvi [1,*]

1 Department of Geography, Government College University Faisalabad, Faisalabad, Pakistan; naqia.gull@gmail.com; drliaqataliwaseem@gcuf.edu.pk; elahiadnan1@gmail.com; aliasadnaqvi12@gmail.com
2 Department of Space Science, The University of the Punjab, Lahore, Pakistan; adeelhr7@gmail.com
3 Department of Computer Sciences, The Karakoram International University, Gilgit-Baltistan, Pakistan; dostdar.hussain@kiu.edu.pk
4 Department of Geography, Government College University Lahore, Lahore, Pakistan; nasir_gis_geo@hotmail.com
5 Manager GIS, IT Department, SSGC Head Office Near Civic Centre, Gulshan-e-Iqbal Karachi, Sindh Pakistan; zawwar.gis2014@gmail.com
6 Department of Mathematics, Dawood University of Engineering and Technology, Karachi; bulbul@duet.edu.pk
7 Department of Geography, Govt. Postgraduate College Gojra, Gojra 56000, Pakistan; nasarbhalli@yahoo.com

ABSTRACT

Background: Land Surface Temperature (LST) is a significant factor for surface processes. Mountain is critical for global energy and mass balance. Deviations of topographic properties of the land surface are causative factors of LST variations.
Objectives: In this study, the spatio-temporal variations in LST are investigated according to changes in elevation, slope, vegetation (Normalized Difference Vegetation Index - NDVI), rainfall, and snowfall (Normalized Difference Snow Index – NDSI). Tehsil Murree, Punjab was chosen as a case study.
Methods: Digital Elevation Model (DEM) and Images of Landsat 8, Sentinel-2A, and MODIS for each month are used to calculate mean seasonal LST for 2017. The slope and elevation of the study area are extracted from DEM while MODIS is used to compute LST. Sentinel-2 images are used to calculate NDVI, and rainfall is collected from PERSIANN-CCS moreover Landsat-8 is used to calculate NDSI. All independent parameters are correlated with dependent-parameter by using linear regression and geographically weighted regression (GWR).
Results: Both models reveal that elevation is the most significantly controlling the distribution of LST. Other variables also influence LST; e.g., rainfall and vegetation (NDVI - third significant influencer) while using linear regression. The vegetation (NDVI) and rainfall (rainfall - last in rank) affect the LST when evaluated via the GWR model. Slope and NDSI in linear regression and GWR also affect the LST respectively. In general, the minimum and maximum temperatures in summer, monsoon, and winter seasons remained 24°C and 36°C (summer), 20°C and 33°C (monsoon), and 14°C and 23°C (winter), respectively. The mean temperatures remained 30°C, 26.5°C, and 18.5°C in summer, monsoon, and winter, respectively.
Conclusions: This study might be helpful to understand the most significant factors affecting LST and to estimate the water stress, flood, and snowline as well to understand the recent trends of global warming in correlation with the seasonal profile in hilly areas.

ARTICLE HISTORY

Received: 13 Jun 2021
Accepted: 29 Jun 2021
Published: 30 Jun 2021

KEYWORDS

Land surface temperature; LST; spatio-temporal variation; spatial dependence; geographically weighted regression; GWR; spatial heterogeneity; mountainous terrain; Pakistan;

1. INTRODUCTION

***CONTACT** Ali Asad Naqvi aliasadnaqvi12@gmail.com

Land surface temperature (LST) is the radiative skin temperature of the land surface (Phan et al., 2018; Sekertekin, 2019). The earth's temperature depends upon the entire radiation that is received from the sun. The absorbed solar radiation is responsible for temperature rise leading to the emission of longwave radiation from the earth's surface. The absorption and emission help regulate the geophysical processes and depend on the surface's thermal characteristics. Changes to the surface temperature can lead to altered energy balance (absorption and emission) that subsequently alter the geophysical cycles (Saher et al., 2019). LST is a significant climatic parameter, associated with the integrated thermal state of the atmosphere and surface energy balance within the external layer of planetary boundary (Sun, 2008). LST controls the longwave radiation that is released by the surface of the earth. Between the surface and the atmosphere, it is also essential for the estimation of the sensible and latent heat fluxes (Trigo et al., 2008).

Many techniques are playing an essential part in controlling the temperature depending on spatial patterns of elevation including snow-albedo feedback, changes in the moisture content of the atmosphere, and radiative forcing at low temperatures. The sensitivity of temperature is also being increased by cloud patterns (Pepin et al., 2019). It is noticed that in complex terrain, the earth's radiation budgets are generated by the topographical variations and electromagnetic radiations of the surface (Oliphant et al., 2003). Most of the studies show that the variations of topographical features (slope, elevation, and aspect) and the physical appearance of land surface for example land cover (LC) types as well as vegetation (normalized difference vegetation index (NDVI)) are causative factors of LST variations. Generally, the latent heat flux rises in woodland flora and minimizes the intensity of LST as compared to scrubland or deserted areas (Pepin et al., 2019). The difference between air temperature and LST is minimized with high vegetation, and it increases humidity because of the increase in latent heat flux (Maeda & Hurskainen, 2014). In employing NDVI, higher values represent the high vegetation fraction. There is a negative correlation between LST and NDVI owing to evapotranspiration (Voogt & Oke, 2003).

Precipitation is a primary meteorological and hydrological variable that has a great impact on weather, climatology, hydrology, and ecosystems. It also affects the global energy and water cycle. It considerably affects the earth's surface energy balance and interactions between atmosphere and land by varying soil moisture (Li et al., 2013). As a result of the high variations in precipitation, obtaining accurate measurements of precipitation on ground-based is challenging (Tustison et al., 2001; Wanders et al., 2015). However, measuring the rainfall (data) has prime importance against various hazards and disasters. For instance, the capability of acquiring high-resolution estimates of geospatial variability in rainfall fields proves significant for the identification of local powerful storms which could lead towards dangerous floods and even flash floods (Goovaerts, 2000).

Hence, the role of LST is crucial for several physical and environmental phenomena and spatio-temporal assessments like this one could help in unveiling the salient factors responsible for its variability and dependence. This study will help to understand the relationship between elevation differences and the other most influential factors on LST in the study area. LST estimation is beneficial in various studies like water stress on the planet, floods, snow lines, water resource management, and a lot of other parameters that are correlated to air temperature and its lapse rate. This work could provide a useful guide related to the urban and rural ecosystems in evaluating the environment of Murree with contemporary geographical technologies.

2. METHODS

This research computes seasonal LST (Summer, Monsoon, and Winter; during 2017) of Tehsil Murree and assesses the influence of other physical-environmental factors on LST. The factors influencing LST include Elevation, Slope, Vegetation (via NDVI), Rainfall, and Snow (via NDSI).

2.1 Study design

Our study is designed to uncover every areal pattern of LST and its influential factors (within the whole Tehsil Murree). The context is to first compute the dynamics through linear regression and then Geographically Weighted Regression (GWR) is employed to check the spatial heterogeneity. This study encompasses three seasons of the year 2017, i.e., Summer, Monsoon, and Winter. For seasonal demarcation, this study combines monthly data layers; Summer – April to June, Monsson – July to September, and Winter – October to March. For calculating the factors, Digital Elevation Model (DEM; https://vertex.daac.asf.alaska.edu/#), Sentinel-2A, Landsat 8, and MODIS are used. The DEM is used for elevation and slope computation whereas MODIS is employed for LST extraction. Sentinel-2A is used for NDVI calculation and Landsat 8 for measuring NDSI. Rainfall is collected from PERSIANN-CCS. The analysis is seasonal based and comparisons are done through linear regression and GWR models.

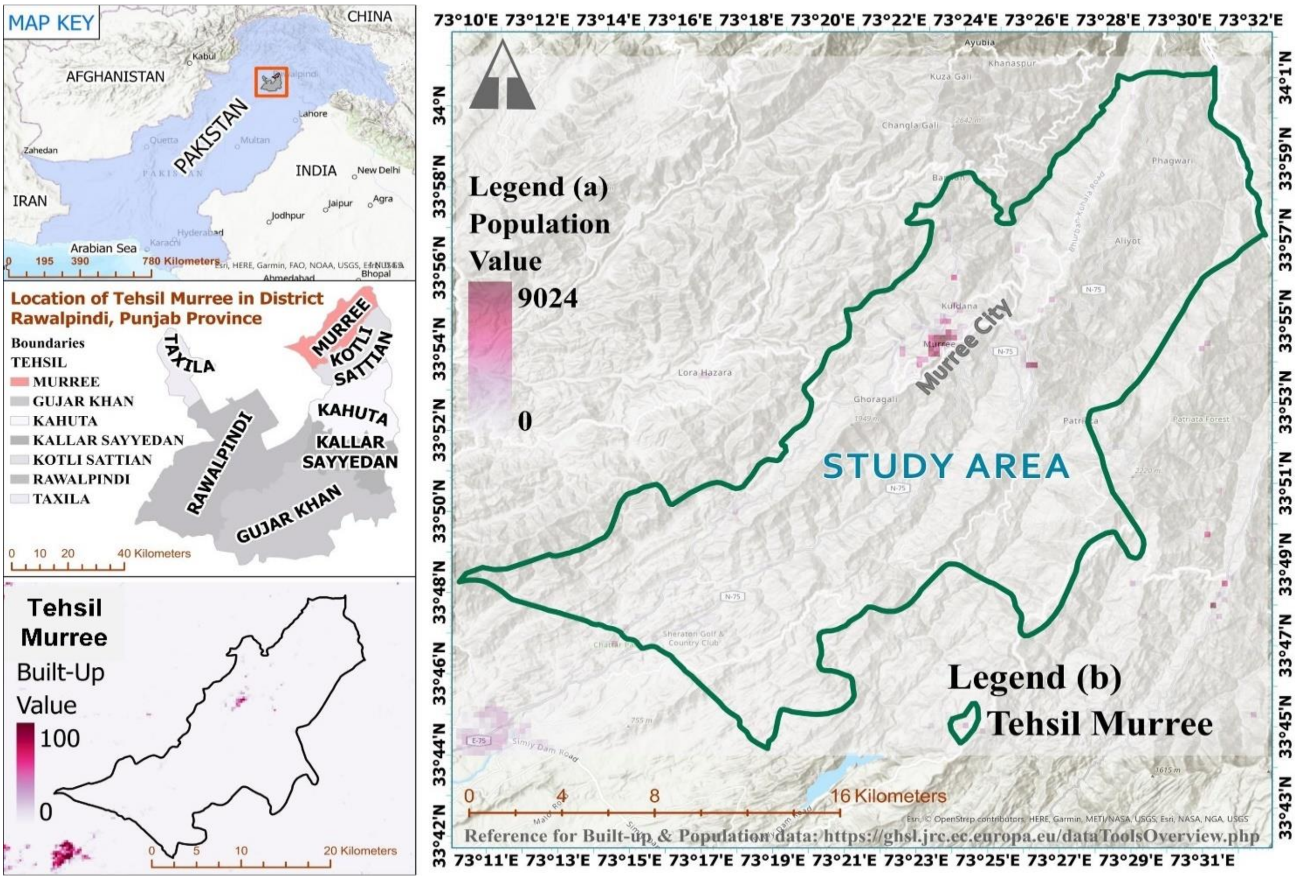

Figure 1. Location map of the study area

2.2 Study area

Murree lovingly called ''the Queen of the hills'', is situated on the southern slopes of the western Himalayan foothills as they arise towards the northeast to Kashmir. Geographically the study area is situated between the 73°10ʹ00ʹʹ to 73°33ʹ00ʹʹ E Longitude and 33°44ʹ00ʹʹ to 34°05ʹ00ʹʹ N Latitude. We have covered the whole Tehsil Murree in our analyses (Figure 1). Murree city (located in Tehsil Murree) is a summer resort (hill station) and tehsil administrative center. It is a subdivision of Rawalpindi District and has the Murree Hills. Murree is situated approximately 50 kilometers northeast of Islamabad which is Pakistan's capital and 87 kilometers from Muzaffarabad (Khan et al., 2011). Physiographically, the altitude of the study area ranges from 3475 meters (highest) to 333 meters (lowest; in the Himalayan foothills) (Figure. 2 d & f). River Jhelum separates the Murree from Azad Kashmir and flows East of Murree. A series of mountain ridges with narrow intervening valleys cover a major part of the area. Within a short distance, there are great altitudinal variations, resulting in very steep slopes and even cliffs. In some areas, through the rock strata, torrential seasonal streams have cut deep gorges. The major part of the watershed comprises steep hills that are hidden under vegetation cover (Hussain et al., 2014).

2.3 Data collection and method to calculating LST

Land surface temperature (LST) products derived from Moderate Resolution Imaging Spectroradiometer (MODIS) are widely used in hydrology, vegetation monitoring, ecology, and global circulation models. The MODIS LST items are made available as a chain of items starting with a swath and advancing to day by day, eight-day, and month-to-month worldwide presented as gridded items by spatial and temporal change (Lu et al., 2018). The product MOD11A1 (MYD11A1) is a Level-3 everyday standard MODIS LST/LSE item with a spatial resolution of 1 km (the accurate grid size is 0.928 km) (Wan, 2015a). The product MOD11A1 is a daily LST product whereas MOD11A2 is a multiday LST product with a 1 km spatial resolution (Wan, 2015b). Other daily-based, eight-day, and month-to-month worldwide LST items are in a geographic projection of the grid cells that display climate modeling. Every one of these products is collected from the MOD11A1 and MOD11B1 daily LST products, and their efficiency relies upon the precision of these two products (Lu et al., 2018; Wang et al., 2015).

This study centers on the reorganization of the LST time series from MODIS. The ongoing research uses the MODIS product (level V006). This level gives better information quality contrasted together with past levels just as other product-based specific upgrades. MODIS Emissivity and Land Surface Temperature products (LST/E;- "MOD11A1" from Terra-satellite &"MYD11A1" from Aqua-satellite) map emissivity values and LST impeccably if there are clear sky situations (Neteler, 2010). The customary methodology utilizing direct interpolation of (regularly meager) meteorological point information has been supplanted here by the elaboration of earlier spatialized satellite maps. For computing LST, we here used MODIS LST product MOD11A2.006 (Figure 2 a, b & c).

2.4 Methods to Determine Elevation and Slope

Digital elevation model (DEM) was used to create elevation (meters) and slope maps (degrees). Digital elevation model (DEM) is essentially the consistent portrayal of a land surface containing XYZ coordinates. A basic map showing elevation was produced by utilizing DEM in ArcGIS 10.5. The maximum gradient between every cell and its neighbors is calculated through slope function. A unique slope value is given to every cell in the output. The low slope represents the flat area, whereas the higher slope represents a steep area. The output dataset can either be calculated as a slope percentage or slope degrees. On the output slope raster, sudden and steep slopes are colored red as Figure 2 e shows. In this study, the slope is calculated using input raster elevation by spatial analyst tool in ArcGIS 10.5 software, which is in degrees.

2.5 Estimation of NDVI

Normalized Difference Vegetation Index (NDVI) was calculated by using Sentinel 2A imageries. NDVI was calculated with the help of frequently used NDVI method/index, presented as follows:

$$\mathrm{NDVI} = \frac{\mathrm{NIR} - \mathrm{Red}}{\mathrm{NIR} + \mathrm{Red}}$$

Where, NIR & Red (spectral bands) are the spectral-reflectance' measurements. These are acquired from near infrared regions and red-visible bands, respectively. The spectral-reflectance are ratios of reflected radiations in each spectral-band; thus, they have values ranging from 0.0 to 1.0. Consequently, the NDVI (values) differs between "−1.0" & "+1.0". Many researchers have established the vegetation threshold as "0.2" (Gandhi et al., 2015) (Figure 3 a, b & c). Areas like sand, barren rocks, or snow usually display very low NDVI values, e.g., 0.1 or less. The moderate NDVI values (Approximately, 0.2 to 0.5) may represent Sparse vegetation, such as senescing crops or grasslands and shrubs. Higher NDVI (approximately, 0.6 to

0.9) values correspond to dense vegetation, such as that found in tropical and temperate crops or forests at their peak growth stage (USGS, 2021).

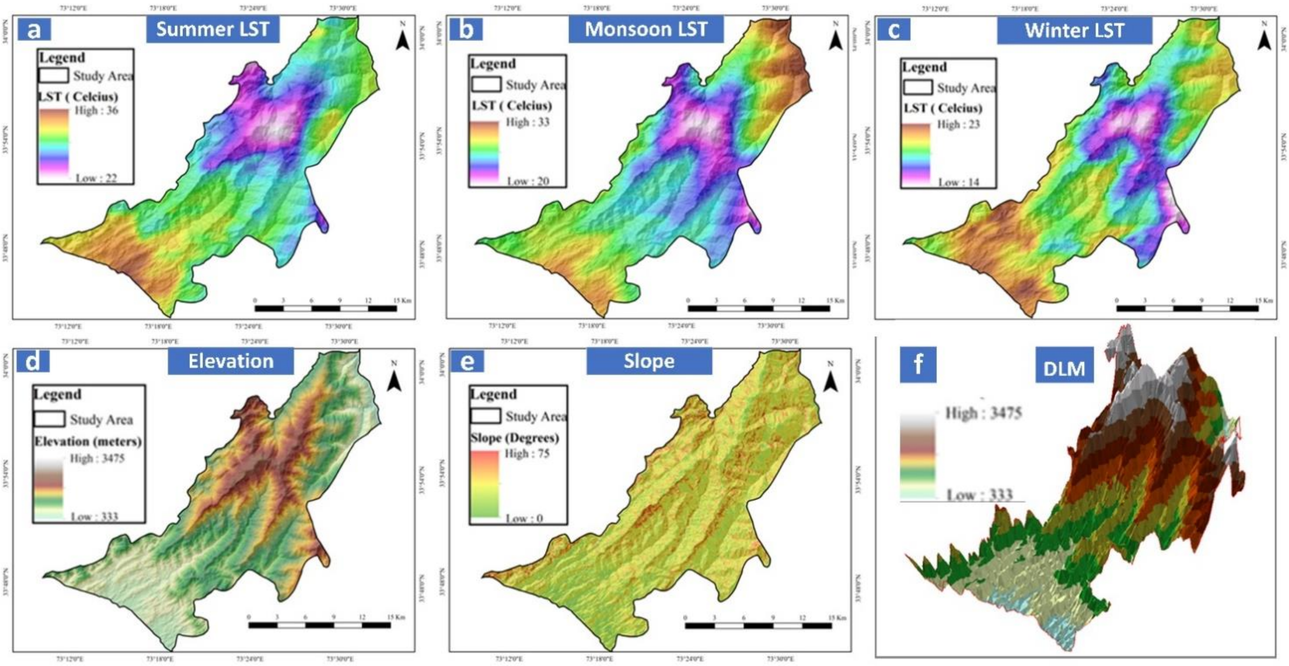

Figure 1. The spatial pattern of land surface temperature (LST) in 2017, Elevation, Slope and Digital Landscape Model (DLM) in Murree, Pakistan: (a) represents Summer LST (b) represents Monsoon LST (**c**) represents Winte r LST (d) Elevation (e) Slope (f) Digital Landscape Model (3D).

2.6 Identification of Rainfall

Rainfall is observed using the PERSIANN-CCS sensor. The PERSIANN-CCS approach consolidates four fundamental strides to determine estimates of precipitation. The initial step is to use a region-growing method and by this method, segmenting the satellite IR cloud images into patches is executed. The next step is to extricate data from the fragmented cloud patches' features, for example, geometry, statistics, and surface at different brightness temperature thresholds. The following stage is to use a self-arranging map (SOM) and sort the cloud patches into distinct clusters. The last step is to devise a relation between the cloud patches' brightness temperature and the rate of rain for every cluster (Mahrooghy et al., 2012). The PERSIANN-CCS categorized varied patches of clouds into various groups and after that, it searches a nonlinear best-mapping capacity for each cluster. This property empowers the PERSIANN-CCS to create different rates of rain, having different brightness temperatures and variable rain/no-rain IR edges for various cloud types. Also, a computerized neural network system for cloud-patch-based precipitation estimation, entitled with Self-Organizing Nonlinear Output (SONO) model is used in it (Hong et al., 2005) (Figure 3 d, e & f).

2.7 Methods to derive Normalized Difference Snow Index (NDSI)

NDSI was observed using Landsat-8 OLI/TIRS data, which provides a good source to calculate the NDSI. The fundamental idea to use optical sensors (Remote Sensing (RS)) for snow mapping/visualization is that snow has a distinctive spectral signature/response. Its reflectance steeply drops in SWIR (Short Wavelength Infrared) and remains lower for longer wavelengths however it has a very high reflectance in visible wavelengths. Thus, the normalized difference (ND) between SWIR and green band (reflectance), is known as NDSI which is widely employed in illustrating/measuring snow (Wang et al., 2015). The NDSI is defined for Landsat 8 OLI (sensor) as:

$$NDSI = \rho green - \rho swir2 \,/\, \rho green + \rho swir2$$

The OLI data product includes a 16-bit quality assessment (QA) file in GeoTIFF format, which contains information on clouds and cirrus. Two tiles were required to cover the study area; a total of 24 images were used to complete this study. Using the ArcGIS mosaic tool, two images of the same month (path number 150 and rows number 36 and 37) were mosaicked, no data values were also removed to extract the correct values of NDSI and clipped the subset raster (Figure 3 g, h & i).

For adjusting spatial resolutions of MODIS and Landsat 8 to Sentinel 2A, we employed the "Resample" tool. After matching pixels, we calculated variable' values and judged the relationship statistically and geospatially. These extracted values were first evaluated through simple linear regression and then prime geographical analysis, namely; GWR.

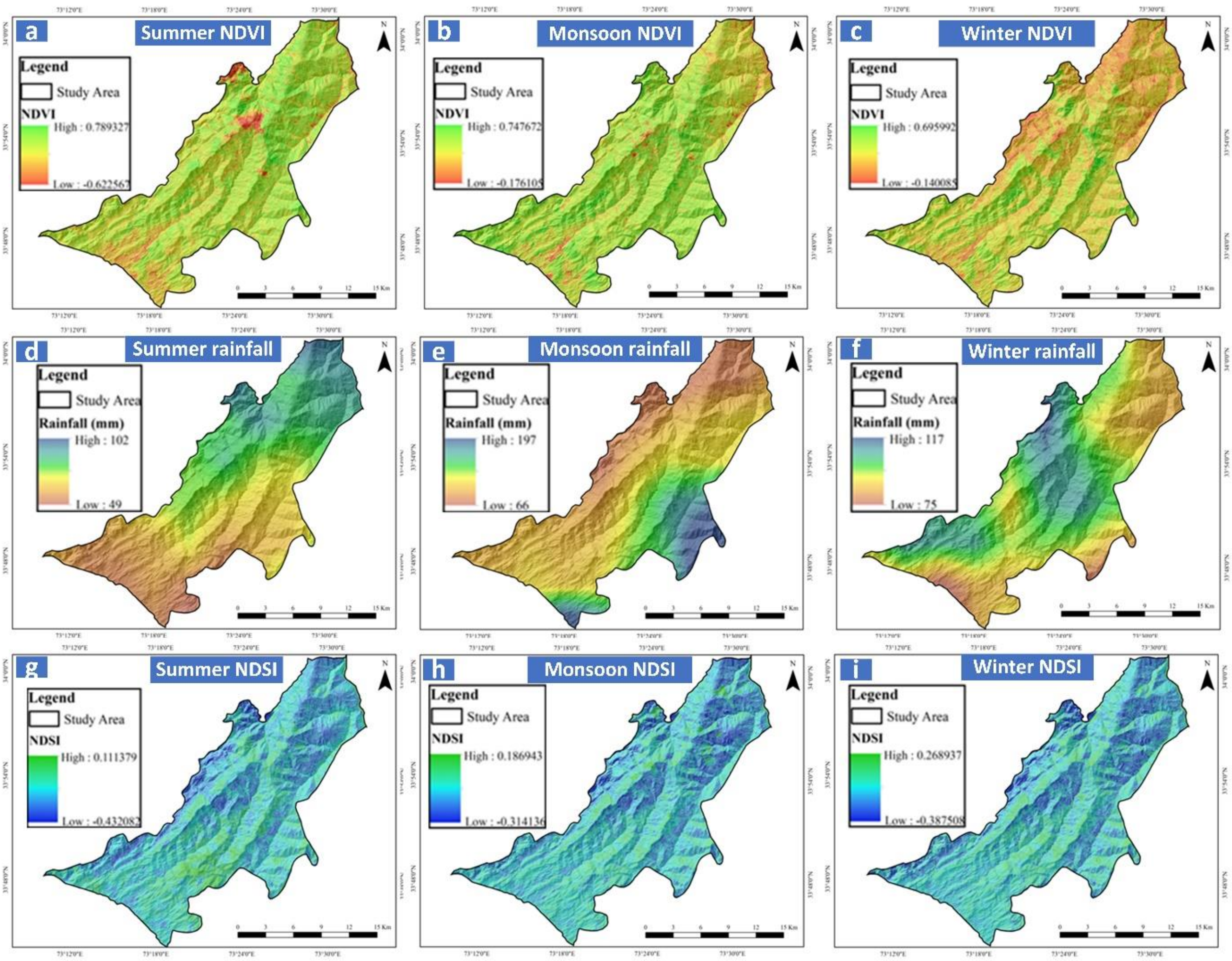

Figure 3. Computation/Visualization of NDVI, Rainfall, and NDSI (2017) for Summer, Monsson and Winter Seasons: (a, b & c) represent NDVI for Summer, Monsson, and Winter Seasons respectively, (d, e & f) represent Rainfall values in millimeters for Summer, Monsson, and Winter Seasons, and (g, h & i) represent NDSI values for Summer, Monsson, and Winter Seasons.

3. RESULTS

In the present study, linear regression analysis has been performed to estimate the connection of LST with different indices including elevation, slope, NDVI, rainfall, and NDSI. Simple linear regression and Geographically Weighted Regression (GWR) analyses were applied to inspect the impact of these factors on LST over Tehsil Murree.

3.1 Relationship between LST and Topographical Factors (TGF)

Two topographical (TG) factors i.e., elevation and slope (degree) have been investigated in this study and their effect on LST has been evaluated in different seasons.
It is evident from Figure 4a,b,c that R^2 values for elevation are 0.63, 0.52, and 0.59 for summer, monsoon, and winter LST, respectively. The higher value for the summer LST season indicates its relatively stronger linear relationship with elevation where 63% of data points fall on the fitted line, showing a strong negative relation. However, very low R^2 values (less than 0.1) for slope in all seasons (Figure 4d,e,f) indicate their weak correlation with LST.

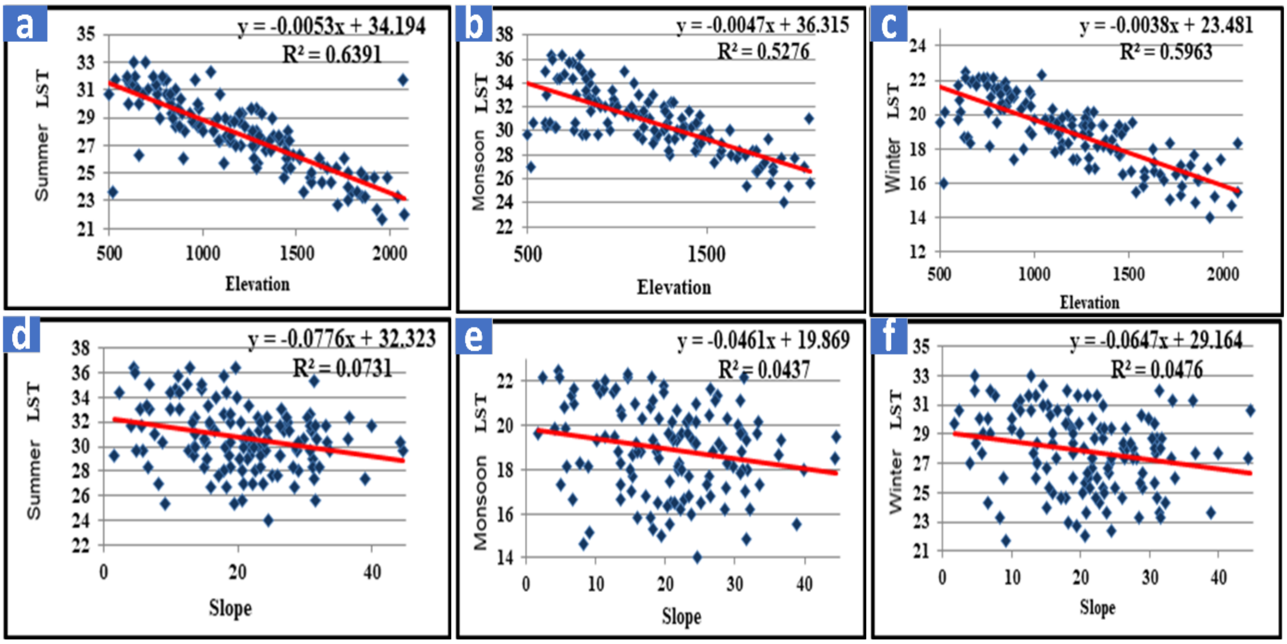

Figure 4. Scatter plots of linear regression model applied: (a, b, and c) represent LST vs elevation during Summer, Monsoon, and Winter seasons. (d, e and f) represent LST vs slope during Summer, Monsoon, and Winter seasons.

Descriptive statistical parameters of these GWR analyses are listed in Table 1, showing that for elevation the residual square values are 37.69, 29.74, and 49.96 which are significantly smaller than the bandwidth of 2892.89, 2735.76, and 3489.304347 for summer, monsoon, and winter season, respectively. It results in the largest effective number and R^2 value for monsoon season and thus having the best-fitted model. The negative trendline in the elevation perspective reflects that LST is decreasing with increasing elevation however weaker relations observed in summer and winter. There could be some thermal anomalies. Such anomalies could be related to the selection of sample points. But those were fixed in the GWR model when R^2 values of ≥0.9 were found, reflecting 90% data values exhibited the best fit in the GWR model for both elevation and slope. The GWR model incorporated spatial heterogeneities effectively even for slope parameter and presented significant relationships among TGF variables even when both i.e., elevation and slope, are compared together with LST.

3.2 Relationship between LST and NDVI (Vegetation)

LST distribution is influenced significantly by vegetation coverage (Waseem et al., 2021). Therefore, to estimate the relation between the amount of vegetation cover and thermal behavior, NDVI is used. To find the relation between NDVI and LST, linear regression and geographically weighted regression techniques were used. In linear regression analysis, we observed (Figure 5 a, b, c) R^2 values of 0.45, 0.60, and 0.41 in Summer, Monsoon, and Winter (comparisons) respectively. We observed a negative trend during all seasons that reflected LST is significantly normalized by vegetation.

Table 1. Descriptive statistics of geographically weighted regression analysis between LST and TGF factors

Variables	Elevation			Slope		
	LST Summer	LST Monsoon	LST Winter	LST Summer	LST Monsoon	LST Winter
Bandwidth	2892.9	2735.8	3489.3	2998.8	2776.5	3193.5
Residual Squares	37.7	29.7	50.0	62.4	48.4	57.0
Effective Number	47.7	51.6	36.3	48.9	54.2	44.9
Sigma	0.7	0.6	0.7	0.9	0.8	0.8
AICc	308.6	290.2	314.5	377.7	362.2	353.8
R^2	1.0	1.0	0.9	0.9	0.9	0.9
R^2 Adjusted	0.9	0.9	0.9	0.9	0.9	0.8
Dependent Field	LST Summer	LST Monsoon	LST Winter	LST Summer	LST Monsoon	LST Winter
Explanatory Field	Elevation			Slope		

GWR results in Table 2, show the non-uniformity in the distribution of R^2 values. There is a significant difference between Residual Square and bandwidth as well as reasonably high values of effective numbers, 59.7, 58.1, and 35.5 for summer, monsoon, and winter LST, respectively. Even the least fitted data points show an R^2 value of 0.9 in winter indicating a good fit for the GWR model. As mentioned above the correlation between NDVI and LST is varied with season, in winter NDVI has a significant influence on LST but less as compared to summer and monsoon while has a negative correlation.

3.3 Relationship between LST and Hydro-metrological Factors (HM)

Analysis of two hydro-metrological (HM) variables such as rainfall and NDSI, was carried out to check their effect on LST. To investigate the relationship between HM factors and LST, the same two techniques i.e., linear and geographically weighted regression was employed. It is evident (Figure 5 d, e, f) that LST shows weak linear relation with Rainfall in all seasons when the observed R^2 values remained 0.25, 0.234, and 0.34 in summer, monsoon, and winter (comparisons) respectively. Interestingly (Figure 5 g, h, i), NDSI exhibited no relation at all in summer and monsoon times however it turned significant in winter with R^2 0.48. The Scatter chart in Figure 5 d, e, f, g, h and i, show quantitatively how the regression line is fitted to data points. They also show the slope and hence dependence between the variables. The largest steepness for rainfall and NDSI in the winter season shows that LST decreases rapidly with the change in these factors. However, LST shows negligible dependence on NDSI in summer. The GWR results for HM factors are presented in Table 3 for rainfall and NDSI. It is observed that R^2 values are non-uniformly distributed spatially. However overall data perfectly follows the GWR model for NDSI where the R^2 value is ≥ 0.9. Whereas, it is down to 0.7 for rainfall in winter (Table 3).

Table 2. Descriptive statistics of GWR analysis of LST and NDVI

Variable	LST Summer	LST Monsoon	LST Winter
Bandwidth	2582.2	2612.2	3744.6
Residual Squares	42.9	44.9	65.3
Effective Number	59.7	58.1	35.5
Sigma	0.8	0.8	0.8
AICc	366.6	367.8	346.8
R^2	1.0	1.0	0.9
R^2 Adjusted	0.9	0.9	0.8
Dependent Field	LST Summer	LST Monsoon	LST Winter
Explanatory Field	NDVI		

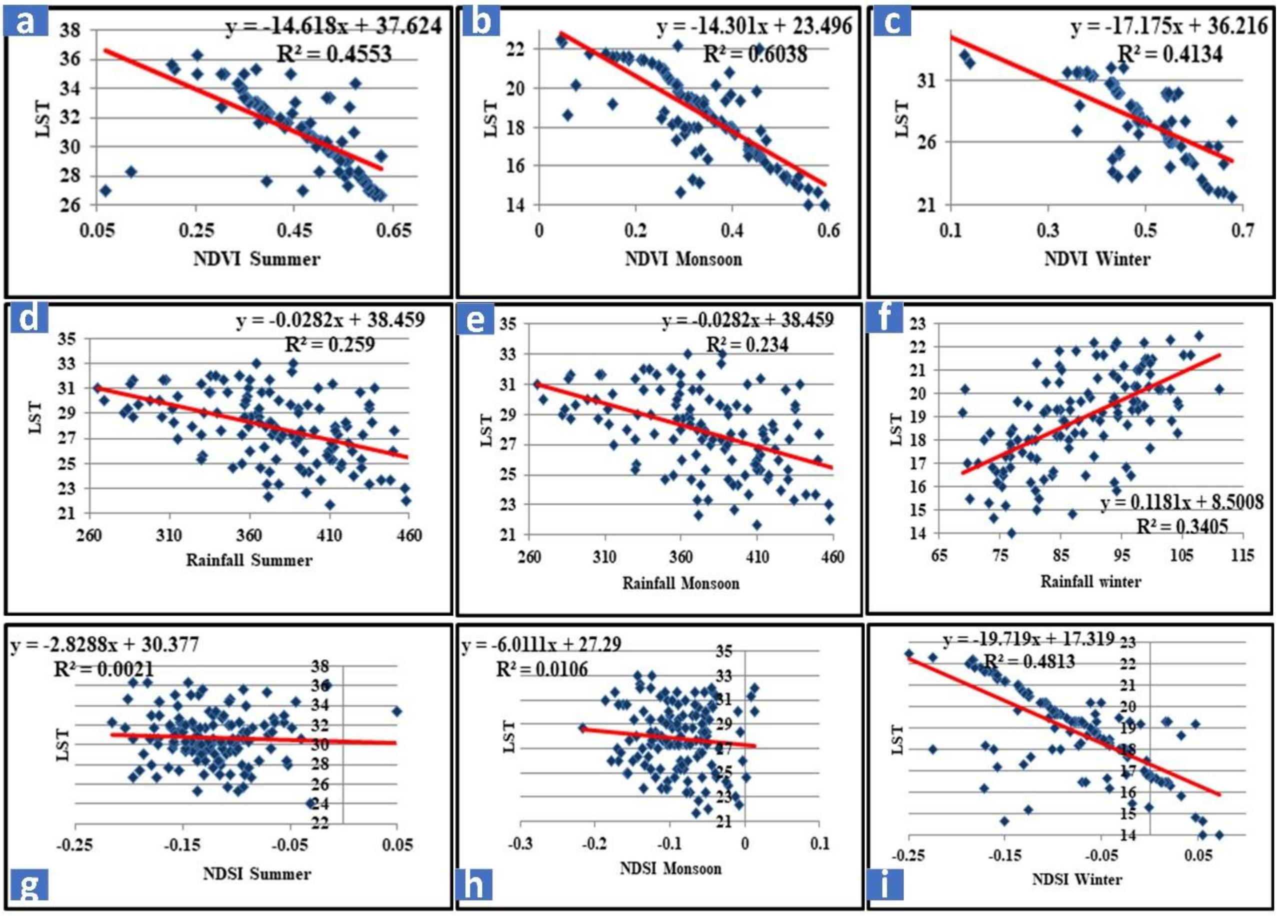

Figure 5. Scatter plots of linear regression model applied: (a, b, and c) represent LST vs vegetation (NDVI) during Summer, Monsoon, and Winter seasons. (d, e and f) represent LST vs rainfall during Summer, Monsoon, and Winter seasons and (g, h, and i) represent LST vs Snow (NDSI) during Summer, Monsoon, and Winter seasons.

Table 3. Descriptive statistics of GWR analysis of LST and HM factors

Variables	Rainfall			NDSI		
	LST Summer	LST Monsoon	LST Winter	LST Summer	LST Monsoon	LST Winter
Bandwidth	6609.0	7211.9	8850.8	2617.2	2630.7	3541.2
Residual Squares	188.9	220.6	167.8	40.2	44.9	67.5
Effective Number	12.5	11.1	8.7	61.6	59.3	39.9
Sigma	1.3	1.4	1.2	0.8	0.8	0.87
AICc	437.6	455.7	416.4	364.1	369.1	360.7
R^2	0.8	0.8	0.7	1.0	0.9	0.87
R^2 Adjusted	0.8	0.7	0.6	0.9	0.9	0.81
Dependent Field						
Explanatory Field	Rainfall			NDSI		

4. DISCUSSION

In this study, we presented analyses of comparative aspects of chosen contributing factors, (in detail) causing variations in land surface temperature (LST) of Tehsil Murree for the period 2017 (one year - Monthly/seasonally). These factors include Elevation, Slope, NDVI, Rainfall, and NDSI (Guha & Govil, 2021; Khan et al., 2020; Leilei et al., 2014; Peng et al., 2020; Thiebault & Young, 2020). Firstly, the LST pattern in Tehsil Murree is analyzed. In general, during the summer season, the minimum and maximum temperatures remained 24º C and 36º C, respectively. In the monsoon season, 20º C was minimum and 33º C was maximum temperature, while in the winter season, the lowest temperature recorded was 14º C and the highest temperature was 23º C as shown in Table 4. The mean temperature was 30º C, 26.5º C, and 18.5º C in summer, monsoon, and winter, respectively (Table 4). The mean temperature was higher in summer and gradually decreased in monsoon and winter seasons.

Table 4. Seasonal mean LST values

Season	Land surface temperature in Celsius (mean)		
	Mini. Temperature	Max. Temperature	Mean Temperature
Summer	24	36	29
Monsoon	20	33	26.5
Winter	14	23	18.5

To examine the relationship of LST with these factors, linear regression and GWR were used; all the parameters have a positive relationship on LST (Alibakhshi et al., 2020; Noi et al., 2017). Elevation has the most influence on LST, rainfall and NDVI also have adequate impacts. The results acquired by linear regression are shown in Table 5.

Table 5. Linear Regression Coefficient between LST and contributing factors

Season	Elevation	Slope	NDVI	Rainfall	NDSI
Summer	0.52	0.07	0.45	0.50	0.00
Monsoon	0.63	0.04	0.60	0.54	0.01
Winter	0.59	0.04	0.41	0.51	0.48

Table 5 shows elevation has a strong positive correlation with LST in all seasons; its correlation coefficient is 52% in summer, 63%, and 59% in monsoon and winter respectively. Rainfall has also greatly influenced LST with R^2 values 0.50, 0.54, and 0.51 in summer, monsoon, and winter seasons respectively. The impact of NDVI on LST is strong in monsoon having a correlation coefficient of 60% but has a weak relationship in summer (R^2 = 0.45) and winter (R^2 = 0.41), comparatively. In the monsoon season, NDSI has the least impact on LST with a correlation coefficient of 01% but in winter has a little bit strong relationship with a correlation coefficient of 48% while has no relationship in summer with R^2 0.0. In the summer and monsoon seasons, the snow index has a negative correlation although in the winter season it has a strong positive correlation with LST (Figure 5). The slope has a weak relationship with LST in all the seasons, e.g., R^2 = 0.07 in summer and 0.04 in monsoon and winter. Overall elevation has great control on LST.

Table 6. Geographically Weighted Regression Coefficient between LST and contributing factors

Season	Elevation	Slope	NDVI	Rainfall	NDSI
Summer	0.96	0.92	0.95	0.76	0.95
Monsoon	0.95	0.94	0.95	0.78	0.91
Winter	0.91	0.88	0.87	0.67	0.86

GWR results represent that in the summer season, rainfall has a relatively weaker relationship with LST (R^2 = 0.76) although elevation has a strong relationship, its correlation coefficient is 96% while NDVI and NDSI have equal correlation coefficient (95%) and slope also has considerable relation as shown in Table 6. In monsoon, elevation and NDVI have equal impact on LST with an R^2 value of 0.95 (Table 6), afterward, slope and NDSI have 94% and 95% coefficients, respectively. In winter, elevation has a strong relationship as in summer and monsoon season, and then slope and NDSI have a great impact on LST with R^2 values of 0.88 and 0.86 respectively. While rainfall has the least impact comparatively in monsoon and winter season as well with R^2 = 0.78 and 0.67 respectively.

LST pattern also analyzed over Tehsil Murree and chosen the locations randomly showed in Figure 2 a, b & c. Generally, it can be observed that temperature is gradually decreasing from north and south towards the central Murree. Meanwhile, the cold zone is located in central Murree from northwest to southeast direction.

Table 6. LST pattern of the study area

Location	LST (° C)	Elevation (m)	Slope (Degrees)	NDVI	Rainfall (mm)	NDSI
Bhanati	21.6	599	9	0.4	196	0.1
Daleh	28	982	42	0.5	247	0.1
Khajut	25.3	1130	46	0.5	265.3	0.3
Phagwari	25.6	1212	34	0.5	251.6	0.3
Bhambrot	25.3	1439	32	0.6	253	0.06
Patraita	22.6	1582	39	0.5	246.3	0.4
Ghora Gali	23.3	1916	23	0.5	252.6	0.3
Murree	21.3	2043	28	0.4	264	0.5
Masoot	21.6	1777	51	0.7	257.7	0.2

As results show that elevation has a strong correlation with LST but other parameters also have impacts, like *Bhanati* is located at 599 m altitude but its temperature is low as compared to *Daleh* that is situated at the elevation of 982 m but has a high temperature (28° C) shown in Table 6. NDVI and rainfall have a weak relation as compared to *Daleh* while NDSIs values are the same at both points. Like this, *Ghora Gali* is at 1916 m in height as compared to *Patraita* by 334 m but has a high temperature because of heavy rainfall (252.6 mm) throughout the year. *Khajut, Phagwari,* and *Bhambrot* are located at different heights between 1100 m to 1450 m but have almost similar temperatures, although at *Bhambrot* NDSI has a very weak relationship with R^2 = 0.06 as Table 6 represents, but has high values for rainfall; 253 mm throughout the year, and has increased in NDVI value by 0.1 correlation coefficient. *Khajut* is situated at 1130 m elevation with 46 degrees of slope angle and *Bhambrot* is at 1439 m height with 32 degrees of slope angle but has the same value of LST. Murree city received heavy rainfall throughout the year that is situated at 2043 m elevation; the highest point of a sample, has the lowest LST of 21.3° C. Overall elevation is a more controlling variable over this study area. Another study has a similar result as elevation is a dominant factor to control the surface temperature (Phan et al., 2018).

Further study may be carried out using both meteorological and satellite data, for example, temperature and rainfall for the 5 years and to estimate the environmental lapse rate using air temperature data from the meteorological department and terrestrial lapse rate using remote sensing data of this study area. In further research, it is recommended to examine the relationship between LST and Normalized Difference Imperviousness Surface Index (NDISI) as well as using multiple daytimes and night-time thermal images can be used to estimate the diurnal and monthly LST variations. Data acquisition based on the satellite images is the main limitation of the study, as the accuracy of data may be affected by an atmospheric error like cloud cover. Because of limited access, data has not to be validated with earth-observed meteorological measurements which is also a limitation of this study

5. CONCLUSION

This study provides an essential insight into the spatio-temporal variability of the LST in mountainous areas of the Tehsil Murree from the perspective of remote sensing observations for the period of one the year 2017. The results show topographical factors on LST are important but also complicated. The regression analysis and GWR indicate that LST values are strongly correlated with mountainous terrain, vegetation index, and hydrological factors.

Linear regression model and geographically weighted regression (GWR) model used to simulate the correlation between dependent and independent variables. Both models indicate that elevation is the dominant variable and control the LST strongly. According to regression coefficient slope has the least impact on LST while a strong correlation is estimated by the GWR model. The vegetation index is also a significant parameter that variates the LST values. The results indicate that NDVI has a strong relationship with LST after elevation, especially in the monsoon season, however, in winter its correlation is a little bit weaker. As shown in Tables 5 and 6, in all seasons NDVI values are higher than the correlation coefficient of 0% that indicates it has a positive relationship with LST. The previous studies show that hydrological factors control the LST as well in complex terrain. Because of high elevation, this area receives heavy rainfall throughout the year while in the winter season snow index has a strong positive correlation.

A more advanced correlation model should also be applied to develop the key controlling factor to examine the accurate temperature pattern in complex terrains. As Figure 2, (d, e, f) shows the physiography of the study is mountainously based, where vegetation index is high and receives heavy precipitation comparatively. Therefore, this study may not be applicable in other types of topography such as the areas that have different climatic types such as plains are coastal areas.

DECLARATIONS

Acknowledgement: We are thankful to the anonymous reviewers for their invaluable feedback that increased the quality of this research article.

Author contributions: Naqia Gull (Data Curation, Formal Analysis, Methodology, Investigation and Writing-original draft). Muhammad Adeel (Software, Analysis, Interpretation, and Visualization). Liaqat Ali Waseem (Interpretation, Methodology and Writing-review and editing). Dostdar Hussain (Writing-review and editing and software). Nasir Abbas (Methodology and Writing-review and editing). Adnan Elahi (Software Support and Data Curation). Zawwar Hussain (Software and Writing-review and editing). Bulbul Jan (Statistical analysis). Muhammad Nasar-U-Minallah (Analysis and interpretation). Syed Ali Asad Naqvi (Idea, Data Curation, Formal Analysis, Methodology, Investigation, Validation, Visualization, Supervision, Writing-original draft, and Writing-review and editing).

Funding: This research work received no external funding.

Conflicts of interest: The authors declare no conflict of interest.

Ethical considerations: This research work does not involve any ethical issues.

Cite this article as;

Gull, N., Adeel, M., Waseem, L.A., Hussain, D., Abbas, N., Elahi, A., Hussain, Z., Jan, B., Nasar-U-Minallah, M., Naqvi, S. A. (2021). Computing Spatio-temporal variations in land surface temperature: A case study of Tehsil Murree, Pakistan. *Journal of Geography and Social sciences, 3*(1), 17-30.

REFERENCES

Alibakhshi, Z., Ahmadi, M., & Farajzadeh Asl, M. (2020). Modeling Biophysical Variables and Land Surface Temperature Using the GWR Model: Case Study—Tehran and Its Satellite Cities. *Journal of the Indian Society of Remote Sensing, 48*(1), 59-70. doi:10.1007/s12524-019-01062-x

Gandhi, G. M., Parthiban, S., Thummalu, N., & Christy, A. (2015). Ndvi: Vegetation Change Detection Using Remote Sensing and Gis – A Case Study of Vellore District. *Procedia Computer Science, 57*, 1199-1210. doi:https://doi.org/10.1016/j.procs.2015.07.415

Goovaerts, P. (2000). Geostatistical approaches for incorporating elevation into the spatial interpolation of rainfall. *Journal of hydrology, 228*(1-2), 113-129.

Guha, S., & Govil, H. (2021). An assessment on the relationship between land surface temperature and normalized difference vegetation index. *Environment, Development and Sustainability, 23*(2), 1944-1963. doi:10.1007/s10668-020-00657-6

Hong, Y., Hsu, K. L., Sorooshian, S., & Gao, X. (2005). Improved representation of diurnal variability of rainfall retrieved from the Tropical Rainfall Measurement Mission microwave imager adjusted Precipitation

Estimation from Remotely Sensed Information Using Artificial Neural Networks (PERSIANN) system. *Journal of Geophysical Research: Atmospheres, 110*(D6).

Hussain, F., Khaliq, A., Irfan, M., & Khan, A. (2014). Morphological and hydrological responses of Soan and Khad rivers to impervious land use in district Murree, Pakistan. *J. Agric. Res, 52*(2).

Khan, A. A., Hussain, D., Ali, K., Khan, G., Ali, M., & Jamil, A. (2020). Time series assessment of the relationship between land surface temperature due to change in elevation: a case study from Hindukush-Himalayan Region (HKH). *Arabian Journal of Geosciences, 13*(13), 515. doi:10.1007/s12517-020-05530-4

Khan, A. N., Collins, A. E., & Qazi, F. (2011). Causes and extent of environmental impacts of landslide hazard in the Himalayan region: a case study of Murree, Pakistan. *Natural Hazards, 57*(2), 413-434.

Leilei, L., Jianrong, F., & Yang, C. (2014). *The relationship analysis of vegetation cover, rainfall and land surface temperature based on remote sensing in Tibet, China.* Paper presented at the IOP conference series: earth and environmental science.

Li, D., Bou-Zeid, E., Baeck, M. L., Jessup, S., & Smith, J. A. (2013). Modeling Land Surface Processes and Heavy Rainfall in Urban Environments: Sensitivity to Urban Surface Representations. *Journal of Hydrometeorology, 14*(4), 1098-1118. doi:10.1175/jhm-d-12-0154.1

Lu, L., Zhang, T., Wang, T., & Zhou, X. (2018). Evaluation of Collection-6 MODIS Land Surface Temperature Product Using Multi-Year Ground Measurements in an Arid Area of Northwest China. *Remote Sensing, 10*(11), 1852.

Maeda, E. E., & Hurskainen, P. (2014). Spatiotemporal characterization of land surface temperature in Mount Kilimanjaro using satellite data. *Theoretical and Applied Climatology, 118*(3), 497-509. doi:10.1007/s00704-013-1082-y

Mahrooghy, M., Anantharaj, V. G., Younan, N. H., Aanstoos, J., & Hsu, K.-L. (2012). On an enhanced PERSIANN-CCS algorithm for precipitation estimation. *Journal of Atmospheric and Oceanic Technology, 29*(7), 922-932.

Neteler, M. (2010). Estimating Daily Land Surface Temperatures in Mountainous Environments by Reconstructed MODIS LST Data. *Remote Sensing, 2*(1), 333-351.

Noi, P. T., Degener, J., & Kappas, M. (2017). Comparison of Multiple Linear Regression, Cubist Regression, and Random Forest Algorithms to Estimate Daily Air Surface Temperature from Dynamic Combinations of MODIS LST Data. *9*(5), 398.

Oliphant, A., Spronken-Smith, R., Sturman, A., & Owens, I. (2003). Spatial variability of surface radiation fluxes in mountainous terrain. *Journal of Applied Meteorology, 42*(1), 113-128.

Peng, X., Wu, W., Zheng, Y., Sun, J., Hu, T., & Wang, P. (2020). Correlation analysis of land surface temperature and topographic elements in Hangzhou, China. *Scientific Reports, 10*(1), 10451. doi:10.1038/s41598-020-67423-6

Pepin, N., Deng, H., Zhang, H., Zhang, F., Kang, S., & Yao, T. (2019). An examination of temperature trends at high elevations across the Tibetan Plateau: The use of MODIS LST to understand patterns of elevation-dependent warming. *Journal of Geophysical Research: Atmospheres, 124*(11), 5738-5756.

Phan, T. N., Kappas, M., & Tran, T. P. (2018). Land Surface Temperature Variation Due to Changes in Elevation in Northwest Vietnam. *Climate, 6*(2), 28.

Saher, R., Ahmad, S., & Stephen, H. (2019). Analysis of Changes in Surface Energy Fluxes Due to Urbanization in Las Vegas *World Environmental and Water Resources Congress 2019* (pp. 175-186).

Sekertekin, A. (2019). Validation of Physical Radiative Transfer Equation-Based Land Surface Temperature Using Landsat 8 Satellite Imagery and SURFRAD in-situ Measurements. *Journal of Atmospheric and Solar-Terrestrial Physics, 196*, 105161. doi:https://doi.org/10.1016/j.jastp.2019.105161

Sun, Y. (2008). Retrieval and application of land surface temperature. *Geo. Utexas. Edu, 1*(1), 1-27.

Thiebault, K., & Young, S. (2020). Snow cover change and its relationship with land surface temperature and vegetation in northeastern North America from 2000 to 2017. *International Journal of Remote Sensing, 41*(21), 8453-8474. doi:10.1080/01431161.2020.1779379

Trigo, I. F., Monteiro, I. T., Olesen, F., & Kabsch, E. (2008). An assessment of remotely sensed land surface temperature. *Journal of Geophysical Research: Atmospheres, 113*(D17). doi:https://doi.org/10.1029/2008JD010035

Tustison, B., Harris, D., & Foufoula-Georgiou, E. (2001). Scale issues in verification of precipitation forecasts. *Journal of Geophysical Research: Atmospheres, 106*(D11), 11775-11784.

USGS. (2021). NDVI, the Foundation for Remote Sensing Phenology. *Remote Sensing Phenology.* Retrieved from https://www.usgs.gov/core-science-systems/eros/phenology/science/ndvi-foundation-remote-sensing-phenology?qt-science_center_objects=0#qt-science_center_objects

Voogt, J. A., & Oke, T. R. (2003). Thermal remote sensing of urban climates. *Remote sensing of environment, 86*(3), 370-384.

Wan, Z., Hook, S., Hulley, G. . (2015a). *MOD11A1 MODIS/Terra Land Surface Temperature/Emissivity Daily L3 Global 1km SIN Grid V006 [Data set]. NASA EOSDIS Land Processes DAAC.*

Wan, Z., Hook, S., Hulley, G. . (2015b). *MOD11A2 MODIS/Terra Land Surface Temperature/Emissivity 8-Day L3 Global 1km SIN Grid V006 [Data set]. NASA EOSDIS Land Processes DAAC.*

Wanders, N., Pan, M., & Wood, E. (2015). Correction of real-time satellite precipitation with multi-sensor satellite observations of land surface variables. *Remote sensing of environment, 160*, 206-221.

Wang, X.-Y., Wang, J., Jiang, Z.-Y., Li, H.-Y., & Hao, X.-H. (2015). An Effective Method for Snow-Cover Mapping of Dense Coniferous Forests in the Upper Heihe River Basin Using Landsat Operational Land Imager Data. *Remote Sensing, 7*(12), 17246-17257.

Waseem, L. A., Khokhar, M. A. H., Naqvi, S. A. A., Hussain, D., Javed, Z. H., & Awan, H. B. H. (2021). Influence of Urban Sprawl on Microclimate of Abbottabad, Pakistan. *Land, 10*(2), 95. doi:https://doi.org/10.3390/land10020095